Supplementary information

Giant thermal rectification efficiency by geometrically enhanced asymmetric non-linear radiation

Seongkyun Kim[a†], *Taeyeop Kim*[a†], *Jaehyun Sung*[a], *Yongjun Kim*[a], *Dongwoo Lee*[a*], *and Seunghyun Baik*[a*]

Affiliations

[a.] School of Mechanical Engineering, Sungkyunkwan University, Suwon 16419, Republic of Korea

[†]These authors contributed equally to this work.

*Corresponding author. Email: dongwoolee@skku.edu, sbaik@skku.edu

The PDF file includes:

Figs. S1 to S12

References

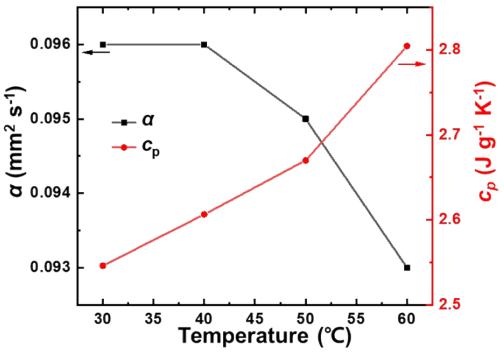

Fig. S1. The thermal diffusivity (α) and specific heat (c_p) of PU.

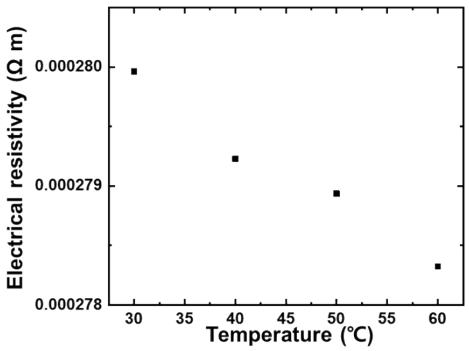

Fig. S2. The electrical resistivity of the Mn film sputtered on a silicon wafer. The electrical resistivity is experimentally measured as a function of temperature by the four-point probe in-line method using a laboratory-built device.[1-3]

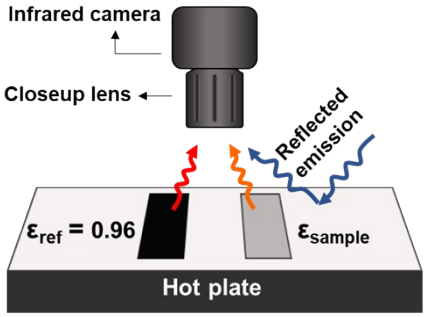

Fig. S3. The reflected temperature and emissivity calibration setup.[4-6]

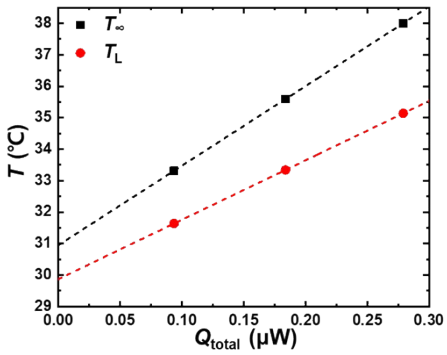

Fig. S4. The experimentally measured environmental temperature (T_∞) and low-end specimen temperature (T_L) are shown as a function of heat flux. The dashed line represents a linear fit to the experimental data.

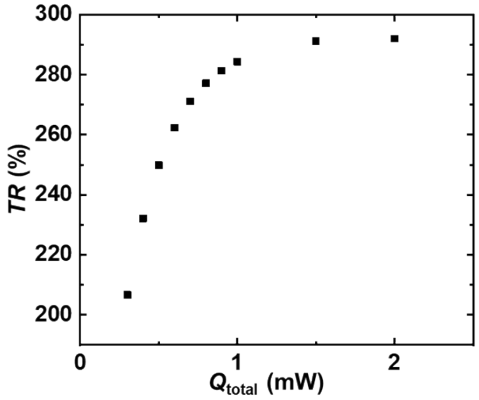

Fig. S5. The thermal rectification efficiency of the asymmetric PU-Mn specimen is simulated by FEM as a function of heat flux (T_L = 35.5 ℃, T_∞ = 38.5 ℃).

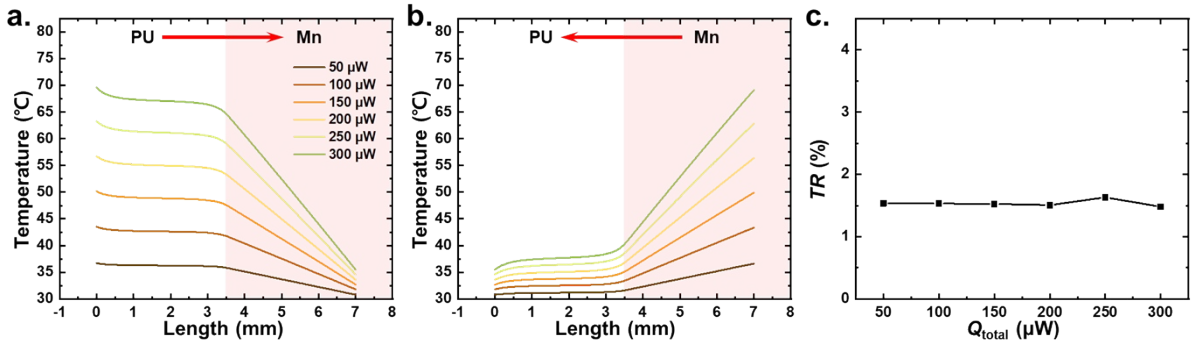

Fig. S6. The temperature profiles (a, b) and *TR* (c) of the asymmetric PU-Mn specimen are simulated considering Q_{cond} only.

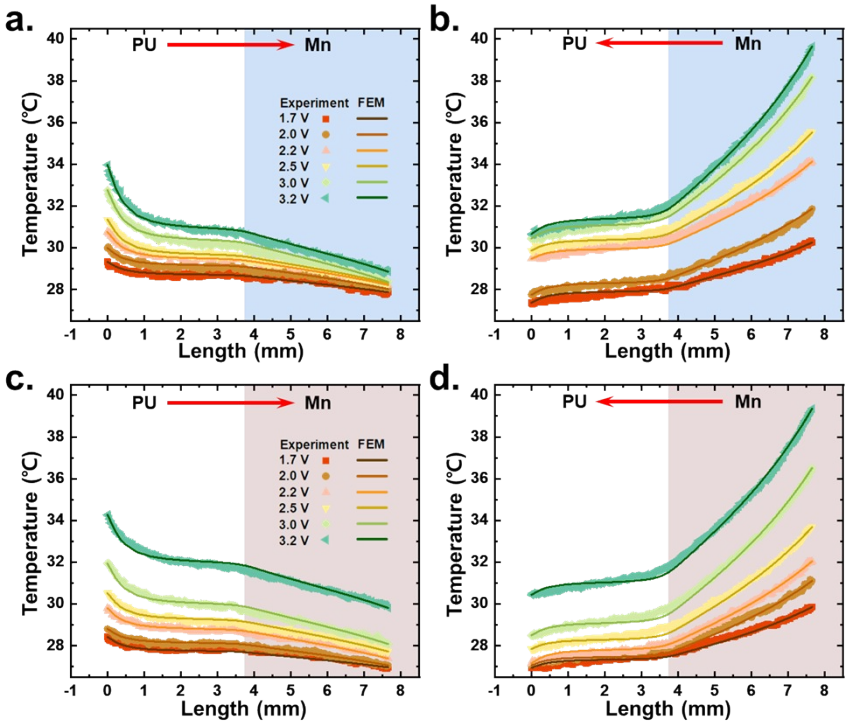

Fig. S7. The temperature distribution along the specimen (applied heater voltage = 1.7 ~ 3.2 V). The FEM simulation result is also shown. The arrow indicates the heat transfer direction. (a, b) The second specimen data. (c, d) The third specimen data.

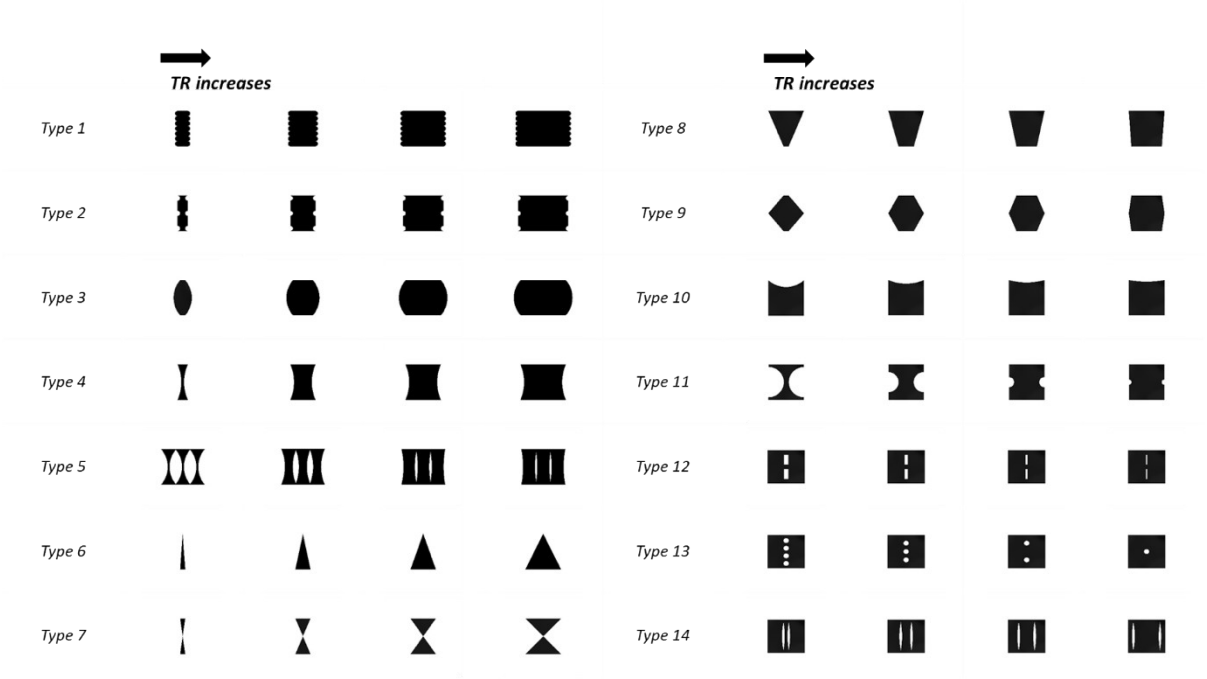

Fig. S8. The representative geometries of 14 different types of thermal rectifiers for the beta-VAE training.

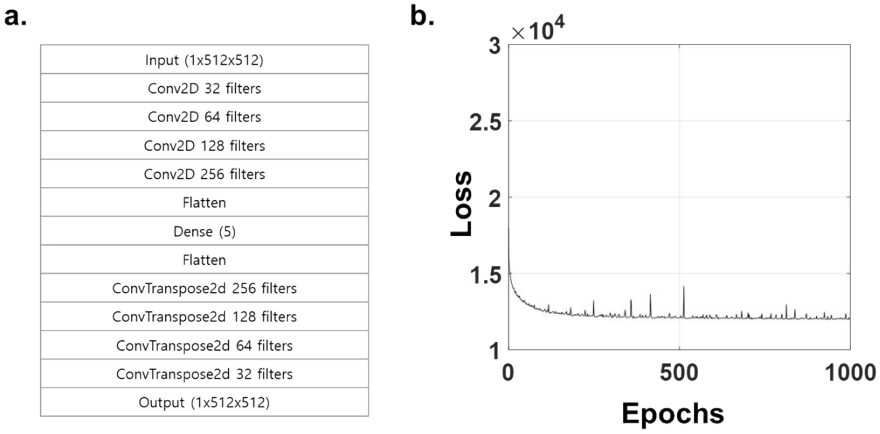

Fig. S9. The details of the beta-variational autoencoder. (a) Structure of the encoder and decoder. (b) Learning history.

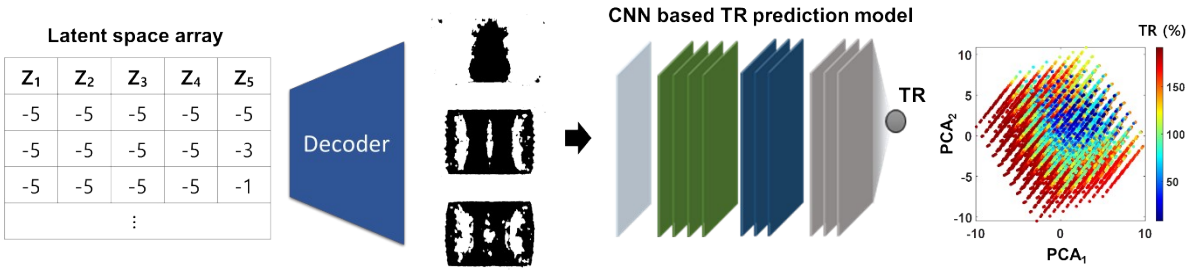

Fig. S10. The proposed framework for the generative designs of asymmetric thermal rectifiers.

a.

Input (1x128x128)
Conv2D 64 filters (3x3)
Conv2D 64 filters (3x3)
Maxpooling
Conv2D 128 filters (3x3)
Conv2D 128 filters (3x3)
Maxpooling
Conv2D 256 filters (3x3)
Conv2D 256 filters (3x3)
Conv2D 256 filters (3x3)
Maxpooling
Dense (4096)
Dense (4096)
Output (TR)

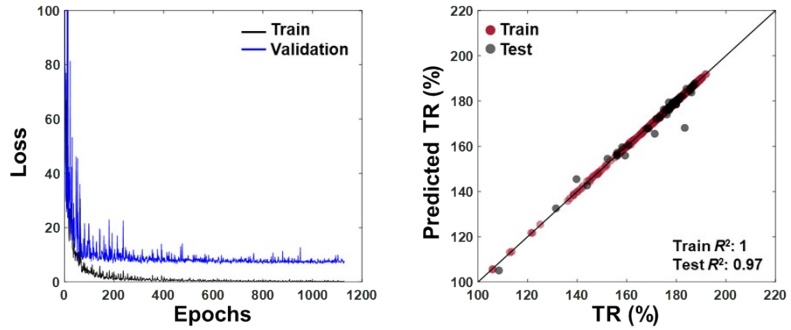

Fig. S11. The CNN-based *TR* prediction model. (a) Structure. (b) Learning history. (c) Training results.

Machine learning prediction	FEM analysis of the simplified design	Error
TR_{ML} = 137 % 	TR_{FEM} = 145 % 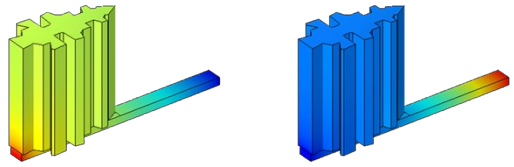	5.8 %
TR_{ML} = 149 % 	TR_{FEM} = 161 % 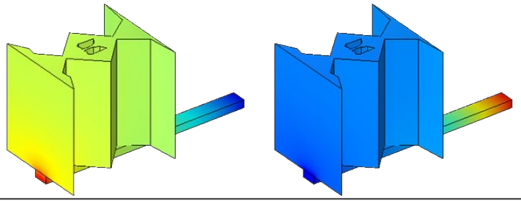	8.1 %

Fig. S12. Comparison of the machine learning prediction (TR_{ML}) and FEM analysis of the post-processed simplified design (TR_{FEM}). The error is calculated by (TR_{FEM}-TR_{ML})/TR_{ML} × 100 (%).

References

1. D. Suh, C. M. Moon, D. Kim and S. Baik, *Advanced Materials*, 2016, **28**, 7220-7227.
2. A. A. Jan, D. Suh, S. Bae and S. Baik, *Nanoscale*, 2018, **10**, 17799-17806.
3. K.-Y. Chun, Y. Oh, J. Rho, J.-H. Ahn, Y.-J. Kim, H. R. Choi and S. Baik, *Nature nanotechnology*, 2010, **5**, 853-857.
4. J. Lee, A. A. Jan, S. P. Ganorkar, J. Cho, D. Lee and S. Baik, *Materials Horizons*, 2021, **8**, 1998-2005.
5. ASTM E1862, Standard Practice for Measuring and Compensating for Reflected Temperature Using Infrared Imaging Radiometers (American Society for Testing and Materials International, West Conshohocken, 2018)
6. ASTM E1933, Standard Practice for Measuring and Compensating for Emissivity Using Infrared Imaging Radiometers (American Society for Testing and Materials International, West Conshohocken, 2018)